Available online at www.sciencedirect.com
SCIENCE DIRECT
ELSEVIER
Tectonophysics 413 (2006) 127–145
TECTONOPHYSICS
www.elsevier.com/locate/tecto

Crustal motion and strain accumulation in western Bulgaria

V. Kotzev [a,*], R. Nakov [b,1], Tz. Georgiev [c,2], B.C. Burchfiel [d,3], R.W. King [e,4]

[a] *Central Laboratory of Geodesy, Bulgarian Academy of Sciences, Acad. G. Bonchev St. Bl. 1, 1113 Sofia, Bulgaria*
[b] *Geological Institute, Bulgarian Academy of Sciences, Acad. G. Bonchev St., Bl. 24, 1113 Sofia, Bulgaria*
[c] *Geophysical Institute, Bulgarian Academy of Sciences, Acad. G. Bonchev St., Bl. 3, 1113 Sofia, Bulgaria*
[d] *Department of Earth, Atmospheric and Planetary Sciences, Massachusetts Institute of Technology, 54-1010, Cambridge 02139, USA*
[e] *Department of Earth, Atmospheric and Planetary Sciences, Massachusetts Institute of Technology, 54-612, Cambridge 02139, USA*

Received 14 December 2004; received in revised form 21 October 2005; accepted 28 October 2005
Available online 27 December 2005

Abstract

Global Positioning System (GPS) data acquired between 1996 and 2004 and fault plane solutions for four seismic zones are analyzed to obtain the velocity and strain rate fields for western Bulgaria. The GPS derived velocities suggest that southwestern Bulgaria moves to the S to SSE at a rate of ~1 mm/year with respect to northern Bulgaria and southern Romania, defining an approximately ESE-trending extensional boundary that marks the northernmost extent of the Aegean extensional domain. The boundary includes the E–W trending Sub-Balkan graben system of central Bulgaria and its westward continuation into the Sofia graben. Active faults within the boundary region trend ENE to WNW, and they have normal or oblique normal and strike–slip displacements consistent with the velocity field. Within the western part of the boundary region, extension is transferred to the north of the Sofia graben across the westernmost part of the Stara Planina Mountains and the ridges of the western Sredna Gora. The geodetically derived N–S extension is in agreement with the seismic data that show a variable pattern, but with projections of the T axes mostly lying within the N–S quadrant. The predominant type of faulting is caused by sub-horizontal extensional stresses in an approximate N–S direction. This is consistent with extension and oblique strike–slip interpreted from geological studies that show numerous WNW, ENE to E–W-trending active normal faults in western Bulgaria.

Keywords: Crustal strain; GPS; Seismicity; Bulgaria; Eastern Mediterranean

1. Introduction

Different types of geological and geophysical data permit the tectonic analysis of crustal deformation over a broad range of time scales. Such analyses present the opportunity to examine the consistency of these data sets to explain the temporal and spatial distribution of deformation and ultimately to form the basis for development of better geodynamic models. In this paper we integrate geological interpretations of faulting in Bulgaria over the past 10^4 to 10^6 years with seismic and geodetic observations in order to understand the relationship between the current strain field and long-term deformation and hence better assess seismic risk.

Bulgaria is located at the northern boundary of the Aegean extensional regime. Most analyses of this regime focus on the area south of the North Anatolian

* Corresponding author. Fax: +359 2 720 841.
E-mail addresses: kotzev@bas.bg (V. Kotzev), radnac@geology.bas.bg (R. Nakov), georgiev@geophys.bas.bg (T. Georgiev), bcburch@mit.edu (B.C. Burchfiel), rwk@chandler.mit.edu (R.W. King).
[1] Fax: +359 2 724 638.
[2] Fax: +359 2 700 226.
[3] Fax: +1 617 252 1800.
[4] Fax: +1 617 253 1699.

0040-1951/$ - see front matter © 2005 Elsevier B.V. All rights reserved.
doi:10.1016/j.tecto.2005.10.040

fault which numerous geological and geophysical studies characterize as early Cenozoic to Recent regional extension bounded by narrow zones of subduction and shortening along the Hellenic trench to the south and west (Fig. 1; e.g., McKenzie, 1972, 1978; Le Pichon and Angelier, 1979). Our geological studies (Burchfiel et al., 2000; Nakov et al., 2001) suggest that the northern boundary of the Aegean extensional regime passes though north central Bulgaria, supporting McKenzie's interpretation based on limited seismic data that a poorly defined crustal boundary passed through that same region (McKenzie, 1972). Our analysis of young and active faulting has indicated that much of the Balkan Peninsula has been characterized by extensional tectonism which we refer to as the southern Balkan extensional region. The tectonic evolution of this region indicates that in the early Cenozoic it was an intimate part of the Aegean extensional regime, but with much less extension from middle Cenozoic to Recent time.

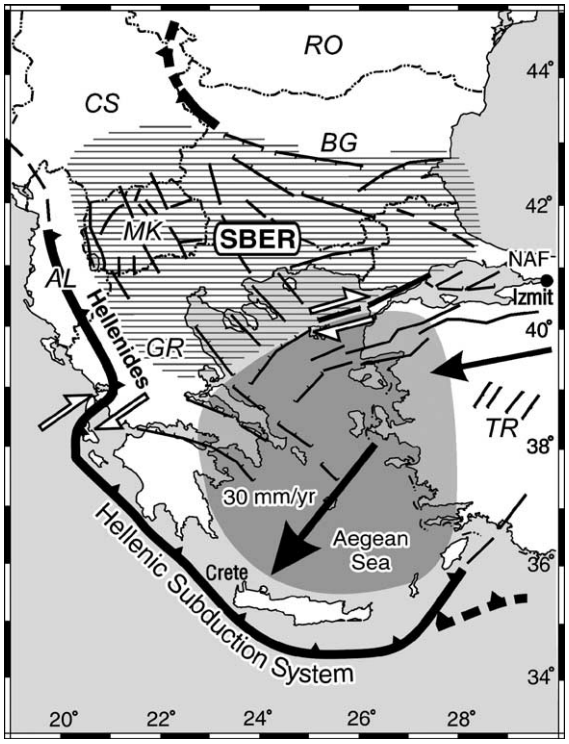

Fig. 1. Simplified tectonic map of the eastern Mediterranean. Arrows show observed direction of motion relative to Eurasia adapted from McClusky et al. (2000). Hatching shows the South Balkan extensional region (SBER). Shaded area indicates the suprasubduction extensional region. NAF is North Anatolian Fault. Solid lines are normal faults, locally with showed down-throw displacement. Lines with triangles are thrust faults. Relative strike–slip displacement is shown with open arrows. Countries: AL, Albania; BG, Bulgaria; CS, Serbia and Montenegro; GR, Greece; MK, Republic of Macedonia; RO, Romania; TR, Turkey.

Only since about 6 Ma it has been separated from the main part of the Aegean regime by the development of the North Anatolian fault.

2. Geological observations

Our tectonic model for the presence of the Southern Balkan extensional region was developed by our geological studies of faults in Bulgaria (Burchfiel et al., 2000; Nakov et al., 2001). Here we examine only the young and active part of the tectonic evolution, classifying faults according to the strength by the evidence for recent activity. In the first category are faults with the strongest evidence for recent displacements from fault scarps, seismic activity and well-developed morphological features. Even for these faults, we have do not have direct evidence for displacement within the last 10,000 years since earthquakes have long recurrence intervals and surface evidence for active faulting is quickly erased. These faults are shown by solid white lines (white in the printed version) in Fig. 2. Second are faults with well-developed morphological evidence that are responsible for present day topography, such as sharp boundaries between basins and mountain fronts, triangular facets and mismatch between the volume of fluvial sediments and the size of the alluvial fans at the base of mountain fronts. These faults we characterize as young faults and probably have had movement within the late Quaternary and may in fact be active. They are shown by grey lines (grey in the printed version) in Fig. 2. In the third category are faults that have more poorly developed morphological features but still bound modern topographic features and often can be shown to cut Quaternary deposits. These faults are shown in black (black in the printed version).

Examination of Fig. 2 shows that most of the active and young faults strike generally E–W, WNW, NW and rarely NE, and that they bound basins of Quaternary sedimentation (Nakov et al., 2001). Most of these are normal faults, a few with strike–slip components. There is a continuous to discontinuous line of faults that trend through central Bulgaria and mostly lie along the south flank of the Stara Planina Mountains. The trend bounds the Sub-Balkan graben system of Tzankov et al. (1996), whose study suggested that the faults dip gently south and have a long-term slip rate of 1–2 mm/year. The faults continue both east to the Black Sea, where they bound narrow and less well-defined half grabens, and west, where they trend into the wide and well-developed Sofia graben. Although seismic activity is present along the bounding faults of the Sofia graben (Figs. 2 and 3), and to the south the Vitosha Mountains rise

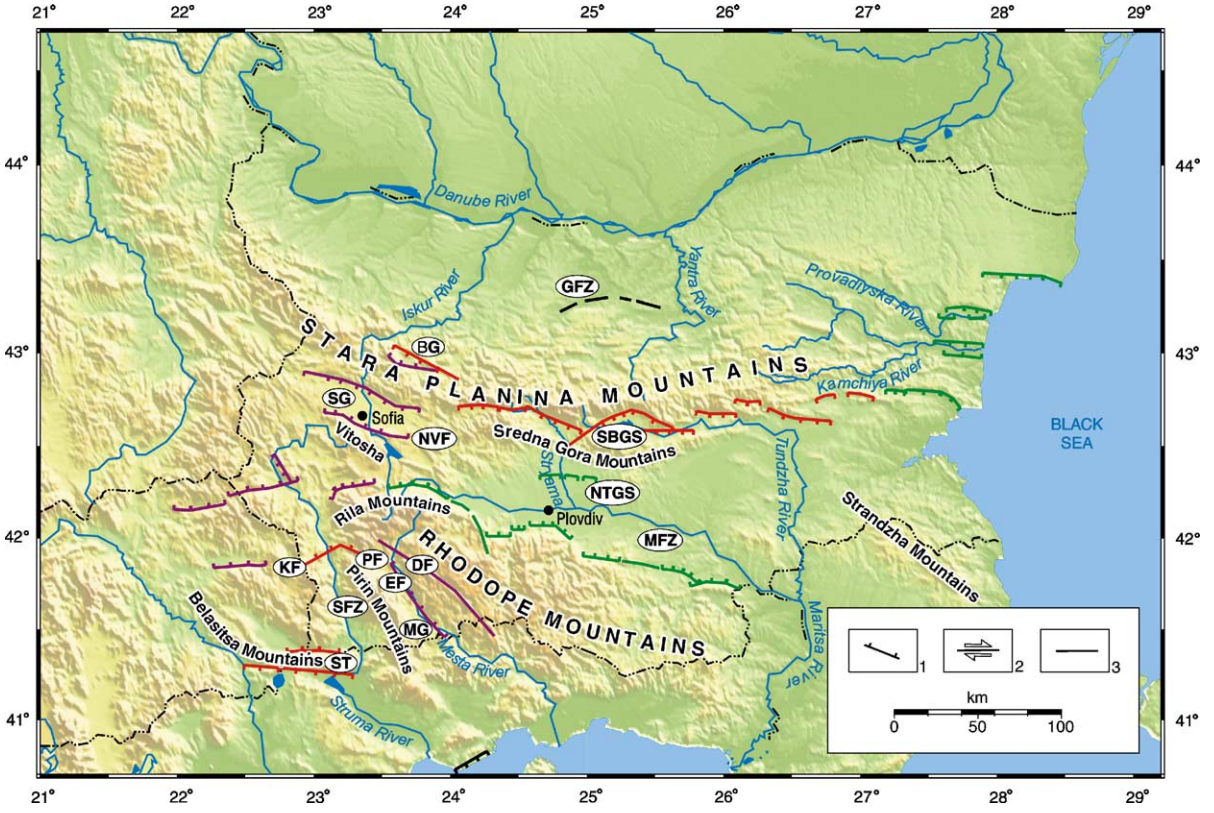

Fig. 2. Topographic map with major extensional structures in Bulgaria. Faults: 1, normal; 2, strike–slip with direction of relative motion; 3, fault with unclear type of displacement. BG, Botevgrad graben; DF, Dospat fault; EF, East Pirun fault; GFZ, Gorna Oriakhovitsa fault zone; KF, Krupnik fault; MFZ, Maritsa fault zone; MG, Mesta graben; NTGS, North Thracian graben system; NVF, North Vitosha fault; PF, Predela fault; SBGS, Sub-Balkan graben system; SFZ, Struma fault zone; SG, Sofia graben; ST, Strumeshnitsa graben. Colors indicate the geological evidence for recent activity (see text).

more than 1000 m above the graben floor, most of the bounding faults fall into category two, without direct evidence of recent displacements. Within the Stara Planina there is one well-developed graben (Botevgrad) that has evidence for an active fault along its north side. North of this belt of faults there is little evidence for significant faulting except for the Gorna Oriakhovitsa fault zone which has earthquake activity but little evidence for surface faulting (this fault is shown in black without white contour in Fig. 2). Hence we interpret the south flank of the Stara Planina Mountains to be the northern boundary for the South Balkan extensional region and the Aegean extensional regime.

The most seismically active fault in Bulgaria is the Krupnik fault in the southwest (Figs. 2 and 3). It is an ENE-striking, north-dipping normal fault with well-developed evidence for active faulting (Meyer et al., 2002). The Predela fault to the east strikes WNW, dips north and lies at the base of a series of triangular facets that forms the northern front to the Pirin Mountains, one of the highest ranges in Bulgaria. The Belasitsa Mountains in southwestern Bulgaria and northern Greece are an active horst marked on both sides of their east end by E–W striking faults.

Also in the southwest are many faults that may be active but with less developed evidence (grey in the printed version) in Figs. 2 and 3). Seismic activity suggests active faulting along the Mesta graben in SW Bulgaria. There is a marked linear belt of NNW-striking faults that bound the east side of the Pirin Mountains, but the faults themselves show little evidence for activity except at their very southern end. Seismic activity occurs north of Plovdiv in the southern part of the North Thracian graben, but in this area of low relief and much human modification of the topography there is little direct evidence for the active faults.

Most of the remaining faults shown in Fig. 2 bound modern day topographic mountain fronts, and while we classify them as young or active, there is only weak evidence to support this interpretation. From field observation the faults are mainly normal, with strikes indicating general N–S extension within most of Bul-

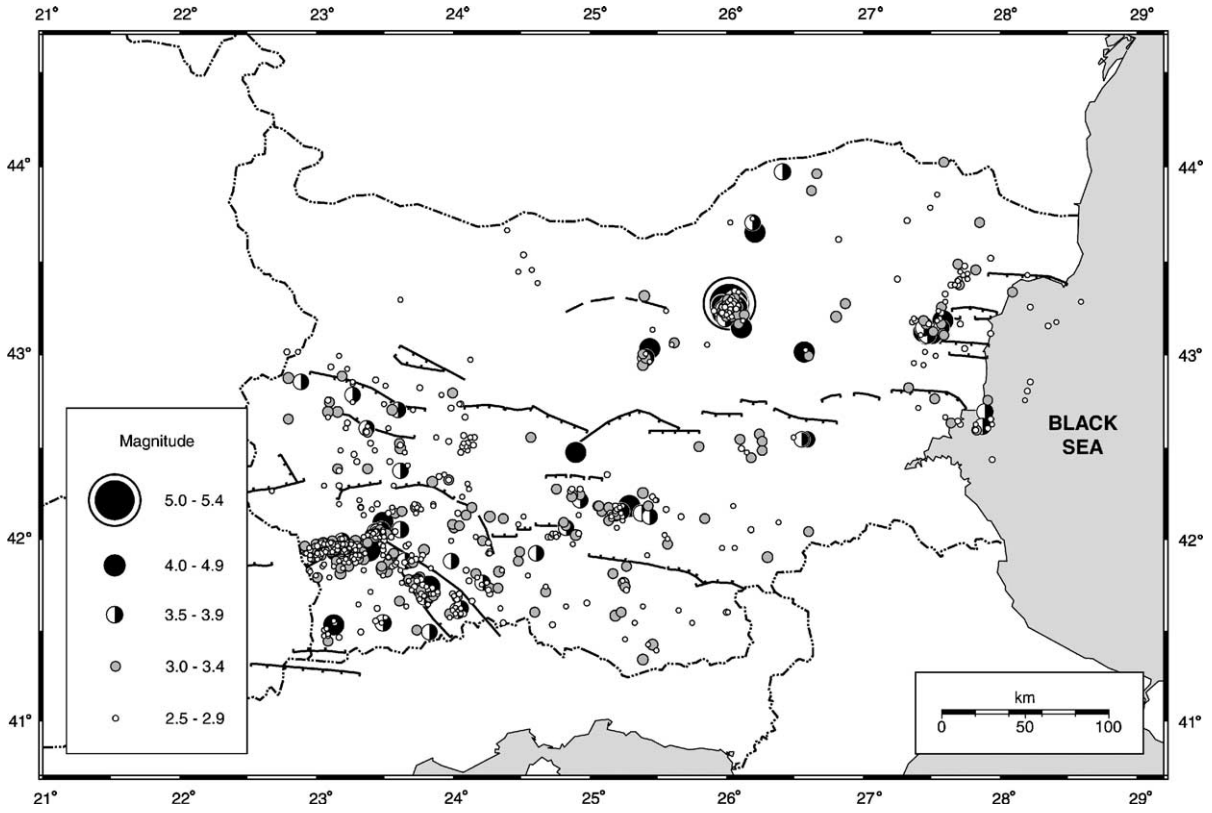

Fig. 3. Earthquakes with magnitudes 2.5–5.4 in Bulgaria between 1981 and 2000 (Botev et al., 1982–2001). Fault symbols used are same as those in Fig. 2.

garia, except for the region north of the E–W-trending Stara Planina mountain range. Individual faults have variations in strike that suggest there may be strike–slip components on the NW- to NE-striking faults. Most of the faults bound mountain fronts, indicating that most of the present day topography of Bulgaria is the result of extensional faulting.

3. Seismological evidence for present-day stress and strain

Historical seismicity in Bulgaria has been documented for the 16th–18th centuries, but more detailed data are available for the 19th century (Shebalin et al., 1974). Seismic activity is not uniform over the country, but is mostly concentrated in the southwest (Fig. 3). One exception is the Gorna Oriakhovitsa seismic zone in central northern Bulgaria with strongest known event of magnitude 7.0 in 1913. In our analysis we group the seismic data into 4 zones: Rila, Rhodope, Plovdiv and Sofia (Fig. 4). The choice of these domains is based on the spatial clustering of earthquakes and to a great extent corresponds to the zonation of Grigorova and Grigorov (1964) who defined seismic zones from their seismic, geological and geophysical characteristics.

The seismic data we examined consist of fault plane solutions for 54 earthquakes with a range in magnitude of 3.0 to 5.7 spanning the period 1956 to 1998. The solutions were obtained by Georgiev (1974, 1982, 1987, 1994) from P-wave first motion polarities taken from NEIC (National Earthquake Information Center), ISC (International Seismological Center), seismic bulletins of neighboring countries, and from revised data from Bulgarian stations. The crustal model assumed by Georgiev for computing the take-off angles, relocation of events, and estimating the focal depths is the same as the model used for compilation of the Bulgaria Catalogue of Earthquakes 1981–1990 (Solakov and Simeonova, 1993). The fault plane solutions are given in Table 1.

To determine regional stresses from the available seismic data, we used the focal mechanism stress inversion package FMSI developed by Gephart (1990). Using the inverse technique of Gephart and Forsyth (1984) stresses that are most consistent with the ob-

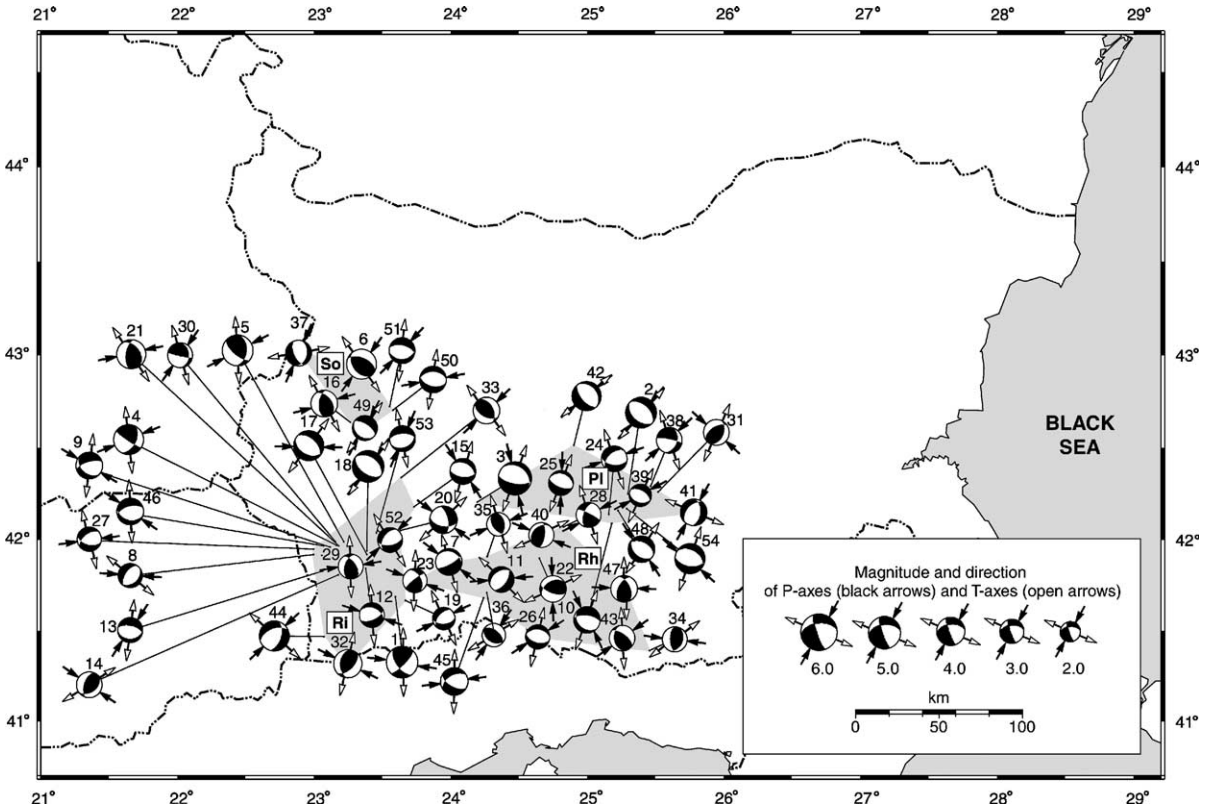

Fig. 4. Fault plane solutions used. The plots are equal-area projections of the lower focal sphere. The strike is defined as the direction of the fault such that the fault plane dips down to the right when looking in the direction of strike. Slip angles vary between 180° and 180° being positive when measured counterclockwise from the horizontal strike direction. Shaded areas show seismic domains: Pl, Plovdiv; Rh, Rhodope; Ri, Rila; So, Sofia.

served focal mechanisms can be determined by assuming that all slip events within a specified volume of the crust reflect a common stress field. The inversion is performed by a grid search over the three stress directions while minimizing the total orientation difference between all of the data and the prediction of the model. In Fig. 5a–d we have shown the P and T axes for each earthquake.

Only 3 of the 4 seismic domains (Rila, Rhodope and Plovdiv) have enough data to develop an adequate interpretation for the stress state. Our results generally confirm the stress tensor inversions of van Eck and Stoyanov (1996) for the Struma and Maritsa fault zones which generally coincide with the Rila and Plovdiv seismic domains.

3.1. Rila seismic domain

The Rila area contains the most data and each fault type when analyzed independently shows a consistent, but somewhat diffuse pattern (Fig. 5a). Normal faults ($n=11$) show a concentration of P axes that cluster near vertical, and T axes that are near horizontal and spread in the N–S quadrants. The general spread of T axes is about 50° on either side of the N–S direction, but most of the data fall within 25°–30° of N–S. Thrust faults ($n=5$) show a concentration of T axes that cluster near vertical, and P axes that are near horizontal and spread in the E–W quadrants at ~30° from E to W. This suggests that the P and T stress axes for the normal and thrust faults reverse their positions, respectively, during different seismic events. It further suggests that the vertical stress is dominant, whereas the P and T horizontal stresses are less strongly oriented in the E–W or N–S quadrants for thrust and normal faults respectively. When strike–slip faults ($n=7$) are added, their P axes generally lie in the E–W quadrants and their T axes lie in the N–S quadrants, both with steeper plunges as expected. The sense of shear on the strike–slip faults is consistent with an overall extension in the N–S direction and shortening in the E–W direction. Thus the overall stress pattern is variable, but with the P axes positioned vertically or their horizontal projections lying in the E–W quadrants, and the T axes positioned

Table 1
Fault plane solutions

No.	Date and time	N^a	Location		H^b	M^c	I Plane			II Plane			T axis		P axis		V^d/H^e	Z^f	F^g	C^h	T^i
			Lat.	Lon.			Strike	Dip	Slip	Strike	Dip	Slip	Az.	Pl.	Az.	Pl.					
1	7205080920	21	41.69	23.60	12	4.9	143.57	58.73	17.05	44.53	75.48	147.57	359.88	32.97	97.09	10.94	0.5/0.8	Ri	I	U	SS[j]
2	7209230153	12	42.25	25.31	10	4.6	132.00	44.00	−90.00	312.00	46.00	−90.00	42.00	1.00	222.00	89.00	1.0/0.0	Pl	II	U	NF[k]
3	7711030222	72	42.20	24.20	15	5.3	306.49	27.93	−66.55	100.34	64.55	−101.91	199.21	18.72	347.18	68.22	1.0/0.2	Pl	II	U	NF
4	7812311626	18	41.97	23.17	10	4.4	27.76	49.53	170.89	123.70	83.08	40.83	354.08	32.96	248.93	21.95	0.7/0.8	Ri	II	A	SS
5	7812311556	22	41.99	23.22	15	4.6	6.50	40.05	139.11	130.04	65.09	57.56	355.83	57.05	243.06	14.09	0.8/0.5	Ri	I	U	TF[l]
6	8003091652	22	42.95	23.35	25	4.4	142.04	41.98	112.84	292.50	51.95	70.75	144.43	74.06	36.04	5.15	0.9/0.3	So	II	U[m]	TF
7	8105060441	14	41.88	23.99	10	3.6	290.71	23.48	−42.87	61.12	74.27	−107.66	165.08	27.19	307.82	57.16	1.0/0.3	Rh	I	U	NF
8	8107171917	11	41.92	23.00	10	3.0	48.69	35.72	−77.82	213.79	55.20	−98.63	309.98	9.82	93.53	77.86	1.0/0.1	Ri	II	A	NF
9	8108261942	19	41.96	23.12	15	3.6	130.96	38.68	−38.79	253.06	66.95	−121.97	5.98	15.97	121.07	55.98	0.8/0.5	Ri	II	U	NF
10	8108301540	15	42.10	25.17	20	3.5	129.58	32.38	−62.81	278.26	61.55	−106.16	20.03	15.09	154.85	69.07	1.0/0.3	Pl	I	A	NF
11	8202200445	13	41.82	24.34	12	3.4	237.33	36.20	−71.29	34.57	55.98	−103.21	134.01	10.08	265.77	75.05	1.0/0.2	Rh	I	A	NF
12	8204270351	16	41.89	23.35	12	3.1	291.47	39.72	−51.69	65.71	59.90	−117.25	174.96	10.91	288.19	63.96	0.9/0.5	Ri	I	U	NF
13	8303112306	15	41.83	23.07	15	3.1	87.45	30.83	−103.16	282.69	60.06	−82.26	7.03	14.73	212.57	73.75	1.0/0.1	Ri	II	A	NF
14	8308130208	15	41.81	23.18	16	3.3	54.16	40.04	118.75	198.54	55.66	67.99	57.48	70.08	304.06	8.19	0.9/0.4	Ri	II	U	TF
15	8309101840	15	42.17	23.73	11	3.4	298.18	36.07	−71.54	95.74	56.05	−102.99	195.03	10.17	327.51	75.12	1.0/0.2	Ri	II	A	NF
16	8312221456	22	42.64	23.27	15	3.6	320.49	44.59	54.15	185.90	55.32	120.00	152.52	64.95	255.09	5.81	0.9/0.5	So	II	U	NF
17	8401100929	18	41.92	23.39	13	4.4	118.84	40.67	−100.16	312.13	50.10	−81.38	36.03	4.75	270.57	81.86	1.0/0.2	Ri	I	U	NF
18	8401231026	30	41.94	23.39	12	4.8	306.00	40.00	−90.00	126.00	50.00	−90.00	216.00	5.00	36.00	85.00	1.0/0.0	Ri	II	U	NF
19	8412071948	14	41.67	23.67	15	2.5	86.27	49.59	−57.72	222.01	49.93	−122.10	334.08	0.18	64.49	66.00	0.8/0.5	Ri	II	U	NF
20	8502160633	22	42.05	23.64	10	3.8	101.23	50.11	−144.79	346.88	63.74	−45.65	46.93	8.09	307.17	50.02	0.7/0.7	Ri	II	U	NS[n]
21	8605151645	28	41.99	23.16	19	4.2	322.53	39.72	51.69	188.29	59.90	117.25	145.81	63.96	259.04	10.91	0.9/0.5	Ri	II	A	TF
22	8705020905	28	41.90	24.65	10	3.5	236.48	39.97	44.01	109.96	63.49	121.08	65.17	59.04	177.95	13.08	0.9/0.5	Rh	II	A	TF
23	8710231825	19	41.78	23.74	10	3.0	331.99	45.35	13.81	232.19	80.22	134.51	181.23	38.10	289.83	22.14	0.7/0.7	Rh	II	U	SS
24	8812230521	18	42.14	25.16	10	3.3	228.17	49.81	−125.01	95.51	51.26	−55.82	162.11	0.80	70.47	63.99	0.8/0.6	Pl	I	U	NF
25	8901160836	17	42.31	24.81	10	3.2	291.00	28.00	−90.00	111.00	62.00	−90.00	201.00	17.00	21.00	73.00	1.0/0.0	Pl	II	U	NF
26	8901180714	17	41.47	24.64	10	3.0	277.50	41.00	−96.34	105.87	49.30	−84.52	191.99	4.16	57.08	84.11	1.0/0.1	Rh	II	A	NF
27	8911281230	16	41.95	23.00	15	3.0	104.61	49.90	−50.81	232.92	53.64	−126.88	348.05	2.08	81.80	61.01	0.8/0.6	Ri	II	U	NF
28	8912061305	15	42.07	24.83	15	3.2	200.01	56.88	169.04	296.05	80.84	33.60	163.24	29.93	63.81	15.89	0.6/0.8	Rh	II	U	SS
29	9003111754	15	41.85	23.27	13	3.2	198.08	48.34	131.39	325.11	55.91	53.38	177.49	60.04	80.12	4.23	0.8/0.6	Ri	I	U	TF

30	9007280928	12	41.97	23.18	10	3.2	358.74	28.85	164.97	101.98	82.81	61.98	343.93	45.06	215.05	32.06	0.9/0.5	Ri	II	U[m]	NF
31	9009101828	12	42.28	25.51	10	3.4	23.90	41.86	64.02	237.09	53.14	111.43	203.61	71.96	312.04	5.88	0.9/0.4	Pl	I	A[m]	TF
32	9101161445	13	41.32	23.25	14	3.9	182.23	43.88	55.51	45.85	55.15	118.57	12.15	66.02	115.97	6.07	0.9/0.5	Ri	I	U	TF
33	9102090856	15	42.34	23.64	10	3.5	332.81	44.85	115.61	118.75	50.51	66.74	324.14	71.99	224.99	2.96	0.9/0.4	Ri	I	A[m]	TF
34	9102172149	16	41.39	25.46	10	3.2	23.00	34.45	110.95	178.10	58.11	76.22	52.76	73.07	278.01	12.10	1.0/0.2	Rh	I	U	TF
35	9103080525	12	41.91	24.27	3	2.8	351.84	45.07	109.89	144.71	48.26	71.17	344.49	75.96	247.91	1.64	0.9/0.3	Rh	II	U	TF
36	9104290401	17	41.71	24.27	10	2.7	120.97	37.52	84.31	308.13	52.70	94.36	239.79	81.64	35.03	7.60	1.0/0.1	Rh	I	U	TF
37	9106171446	16	43.01	22.89	16	3.3	10.91	36.11	−60.45	155.85	59.16	−109.78	260.02	12.05	23.87	69.03	0.9/0.3	So	II	U	NF
38	9109150719	13	42.29	25.46	10	3.4	22.29	39.33	−165.94	281.32	81.14	−51.52	342.02	25.98	226.98	40.98	0.8/0.6	Pl	I	U	NS
39	9109090925	13	42.24	25.39	10	2.5	108.00	37.36	−99.82	300.29	53.28	−82.58	25.00	8.00	242.04	80.01	1.0/0.1	Pl	I	A	NF
40	9203071248	11	42.03	24.67	14	3.1	229.79	30.01	128.60	7.12	66.99	70.18	245.59	62.71	111.86	19.63	0.9/0.3	Rh	II	U	TF
41	9208080252	14	42.15	25.78	16	3.6	220.63	45.82	−64.64	6.41	49.60	−113.79	112.99	1.98	209.10	72.00	0.9/0.4	Pl	I	A	NF
42	9208242143	22	42.51	24.91	20	4.2	320.00	30.00	−90.00	140.00	60.00	−90.00	230.00	15.00	50.00	75.00	1.0/0.0	Pl	I	U	NF
43	9302120253	15	41.46	25.26	9	3.4	172.99	35.79	129.99	307.03	63.38	65.14	176.26	62.92	54.94	14.88	0.9/0.4	Rh	I	U	TF
44	9312160922	34	41.47	23.08	10	4.5	248.01	49.28	−51.92	17.79	53.37	−125.62	132.13	2.26	226.39	62.02	0.8/0.6	Ri	II	U	NF
45	9401110159	14	41.68	24.24	10	3.7	240.12	49.73	−136.44	118.54	58.28	−49.46	181.07	4.89	83.78	55.98	0.8/0.7	Rh	II	A	NF
46	9408030352	18	41.97	23.07	17	3.6	103.16	36.18	−67.15	255.60	57.05	−105.85	356.93	10.72	124.73	72.83	1.0/0.3	Ri	II	U	NF
47	9411261922	15	41.75	25.27	10	3.6	333.86	52.39	48.03	209.70	53.92	130.96	180.70	58.00	272.08	0.86	0.8/0.7	Rh	II	U	TF
48	9411291018	13	42.16	25.22	9	3.6	130.76	42.57	−80.40	297.82	48.17	−98.71	33.98	2.81	147.34	82.93	1.0/0.2	Pl	II	U	NF
49	9512141625	11	42.61	23.37	10	3.2	128.34	27.12	−85.49	303.29	62.97	−92.30	34.99	17.94	208.01	71.93	1.0/0.0	So	II	U	NF
50	9604201956	22	42.70	23.58	8	3.6	270.09	42.85	−101.27	105.30	48.17	−79.72	188.04	2.68	78.83	81.90	1.0/0.2	So	I	U	NF
51	9604202002	20	42.72	23.56	3	3.3	86.75	35.11	−103.44	283.04	55.98	−80.72	6.37	10.54	223.26	76.91	1.0/0.2	So	II	U	NF
52	9710030020	14	42.05	23.47	10	3.1	215.30	44.09	−124.51	79.05	55.02	−61.24	149.05	5.88	45.70	65.96	0.9/0.5	Ri	I	U	NF
53	9711260846	14	42.04	23.46	6	3.4	67.32	32.70	−106.14	266.30	58.74	−79.88	348.97	13.18	203.36	74.15	1.0/0.2	Ri	II	U	NF
54	9812110920	32	42.17	25.29	16	4.5	298.80	41.90	−76.08	100.38	49.59	−102.18	198.98	3.90	311.59	79.95	1.0/0.2	Pl	II	U	NF

[a] Number of signs (compression or dilatation).
[b] Depth in kilometers.
[c] Body wave magnitude.
[d] Vertical component of slip.
[e] Horizontal component of slip.
[f] Seismic zones: Pl, Plovdiv; Rh, Rhodope; Ri, Rila; So, Sofia.
[g] Fault plane.
[h] Choice of rupture plane (Gephart and Forsyth, 1984): A, ambiguous; U, unambiguous.
[i] Type of faulting.
[j] Strike-slip faulting.
[k] Normal faulting.
[l] Thrust faulting.
[m] Rotated auxiliary plane has wrong sense of slip.
[n] Normal faulting with a small strike-slip component.

vertically or their horizontal projections lying in the N–S quadrants. The greatest concentration of T axes is oriented generally N–S, with either the T or P stress axis near vertical.

The orientation of T axes for the normal faults is generally consistent with the orientation of active faults in the northern part of the Rila domain. The Krupnik fault strikes ENE and the Predela fault strikes WNW (Fig. 2). The two different strikes for these faults may be responsible for the spread of T axes determined from the seismic data. In April 1904 the Krupnik fault was the locus of one of the strongest earthquakes during the past two centuries in Europe (Vatsov, 1905). The magnitude of the earthquake was estimated to be between 7.3 and 7.8 by Gutenberg and Richter (1954) and Christoskov and Grigorova (1968). Using satellite imagery and geological data Meyer et al. (2002) found that the possible rupture of the Krupnik fault compatible with their observations would account for a magnitude 6.9 significantly smaller than the previous estimates. Geomorphic features along the Predela fault suggest a dominance of normal faulting with a component of strike–slip (Burchfiel et al., 2000). Even though there are other major mapped faults along the Struma Valley, within the Pirin Mountains to the east, and along the Strumeshnitsa graben, there are no studies that show active faults related to the thrust component of many of the strike–slip focal mechanisms.

3.2. Rhodope seismic domain

The Rhodope domain (Fig. 5b) has fewer seismic events, but the pattern of stress axes is similar to that of the Rila domain. P and T axes for normal and thrust faults, respectively, are oriented near vertical. P axes for thrust faults ($n=7$) lie near horizontal and spread in the E–W quadrants (with one exception), whereas, T axes for normal faults ($n=3$) lie near horizontal and in the N–S-quadrant. No active faults have been mapped in the heavily vegetated mountains in this domain. Only the WNW-striking Dospat fault (Fig. 2) appears to be

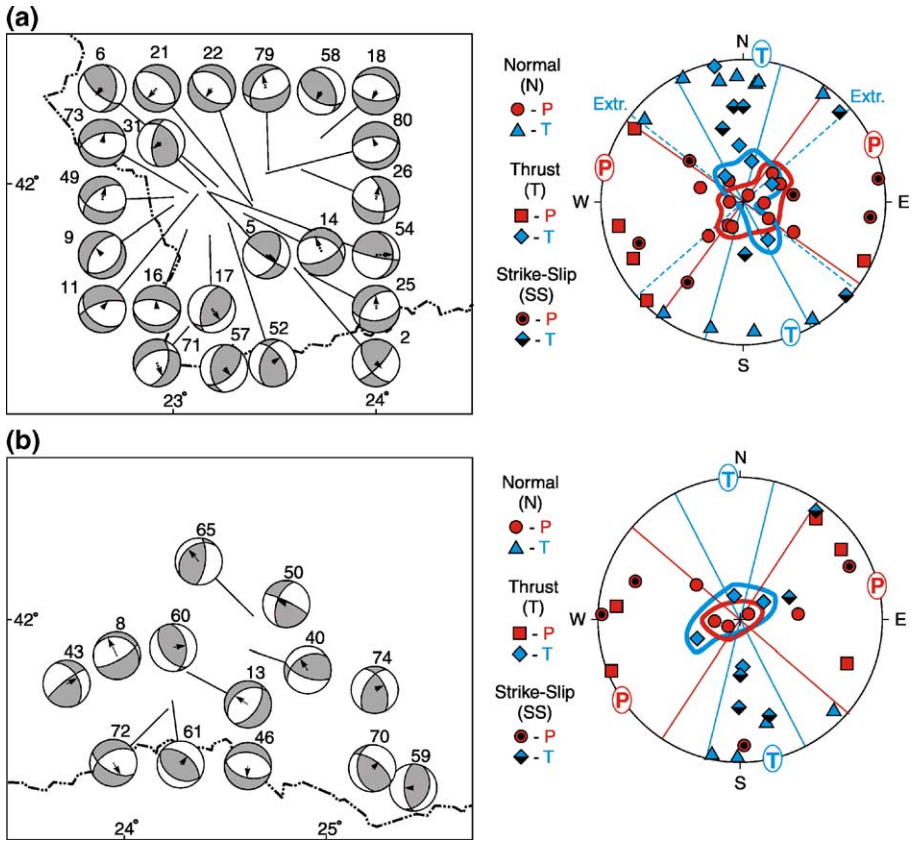

Fig. 5. Stress tensor inversions for seismic zones: (a) Rila; (b) Rhodope; (c) Plovdiv; (d) Sofia. Slip vectors for the chosen nodal plane from each focal mechanism are shown with dash arrows. To the right are shown the maximum (P) and minimum (T) principal stress axes determined from the fault plane solutions. They are keyed by fault type.

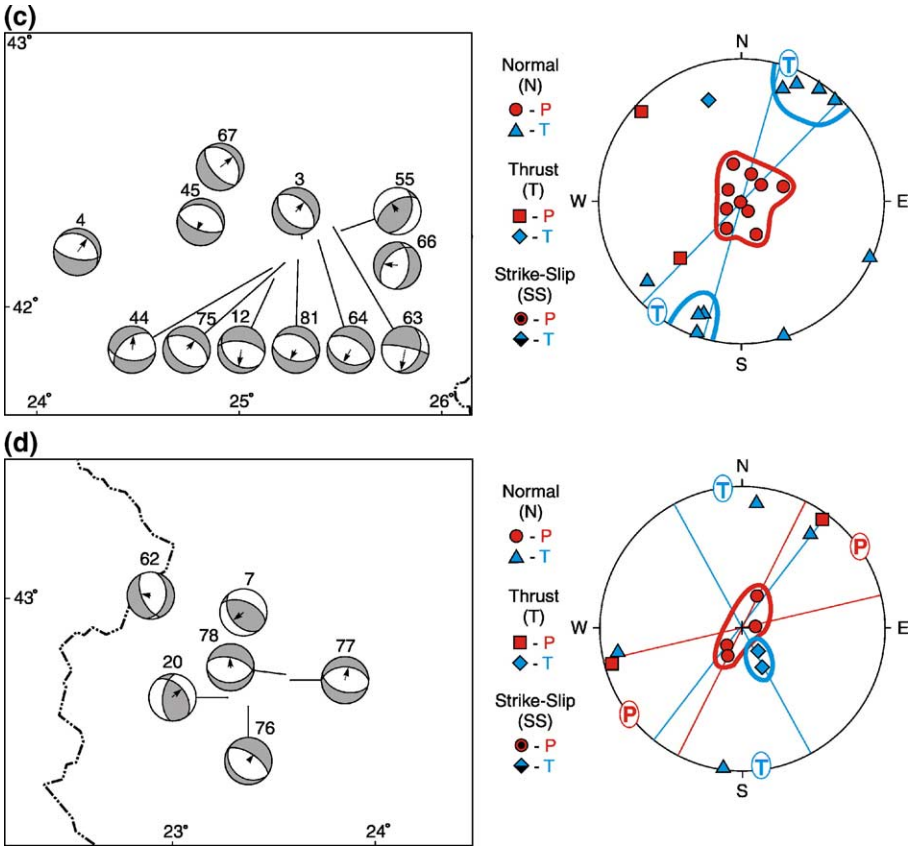

Fig. 5 (*continued*).

an active fault with a probable, but undetermined, strike–slip component.

3.3. Plovdiv seismic domain

The Plovdiv domain contains a predominance of normal faults ($n=8$) with P axes near vertical and T stress axes spread narrowly near horizontally in the N–S quadrants (Fig. 5c). The greatest concentration of T axes lies along a sector N20–40°E. Thrust faults, one with an important strike–slip component, are rare ($n=2$) and show an orientation of principal axes that can be interpreted similarly to the Rila and Rhodope domains, but with few data the correlation is weak. The epicenters of most of the normal fault earthquakes lie within or close to the WNW-trending Maritsa fault zone (Fig. 2), an expected result, since most studies of this region relate seismicity to the active Maritsa fault zone (Kirov and Grigorova, 1961; Stoyanov et al., 1984; Shanov, 2000). Three fault plane solutions indicate NNE-striking faults (Georgiev, 1994) along which magnitude 6.8 and 7.0 earthquakes took place in 1928 (Michailovic, 1933). Faults with N to NNE strike are known in the subsurface of the North Thacian graben (Fig. 2) (Bonchev and Bakalov, 1928), but evidence for surficial active displacement is rare in this generally low rolling vegetated terrain.

3.4. Sofia seismic domain

The Sofia domain (Fig. 5d) has limited data, but the reversal of P and T axes for normal ($n=4$) and thrust ($n=2$) faults, respectively, in a near vertical position is similar to the other domains (Fig. 5d). Corresponding T ($n=4$) and P axes ($n=2$), respectively, are oriented subhorizontally suggesting that the T and P axes have likewise alternated in orientation, but the few data only weakly support this interpretation. The strike of normal faults in the Sofia graben, such as the North Vitosha fault, is dominantly E–W to NW consistent with the normal fault mechanisms. However, geological evidence for thrust faults of the same general orientation is unknown.

4. Geodetic evidence for strain

We have estimated velocities for ~80 GPS stations in the southern Balkan region (Figs. 6 and 7; see also Burchfiel et al., 2005—this issue), combining their data with those from the global network of the International GPS Service (IGS). We established a Bulgaria-wide network in 1996 to study the regional tectonics (Kotzev et al., 2001a). It was fully measured during 3 surveys between 1996 and 2001 (Table 2). In 1997, we augmented these stations with a denser network in western Bulgaria to monitor the strain accumulation in and around the Sofia graben (Figs. 2 and 7; Kotzev et al., 2001b), measuring this network in 1997, 2000, and partly in 2002, 2003 and 2004. For all of these surveys except 2002 and 2004, we occupied station PLA1 at the Geodetic Observatory Plana in order to provide a consistent local reference point. We have also included in our analysis data acquired in 1996 and 2000 in the Republic of Macedonia by the State Department for Geodetic Survey in Skopje and the Bundesamt fur Kartographie und Geodasie (BKG) in Frankfurt, and between 1996 and 2002 in Albania by BKG and the Department of Geodesy of the Faculty of Construction Engineering in Tirana. The regional velocity field used for our tectonic analysis includes the IGS stations near Sofia, Bulgaria, and Bucharest, Romania.

GPS stations in SE Bulgaria surveyed since August 1999 were significantly affected by the $M=7.4$ earthquake on the North Anatolian fault (Fig. 1) near Izmit, Turkey. To improve the velocity estimates for these stations we corrected the offsets using the predictions from the co-seismic model developed by Reilinger et al. (2000) (R. Burgmann, personal communication, 2003). The predicted offsets were 20 mm for AHTG, 7–12 mm for TOPO, BURG, and VATG, 4–5 mm for TSAR and SHUM, and 2–3 mm for MOMC, PLDV, and GABR.

We analyzed the GPS data using the GAMIT/GLOBK software (King et al., 2003; Herring, 2003) and the approach described by McClusky et al. (2000), first combining the regional and global observations for each day into estimates of position for each survey, and

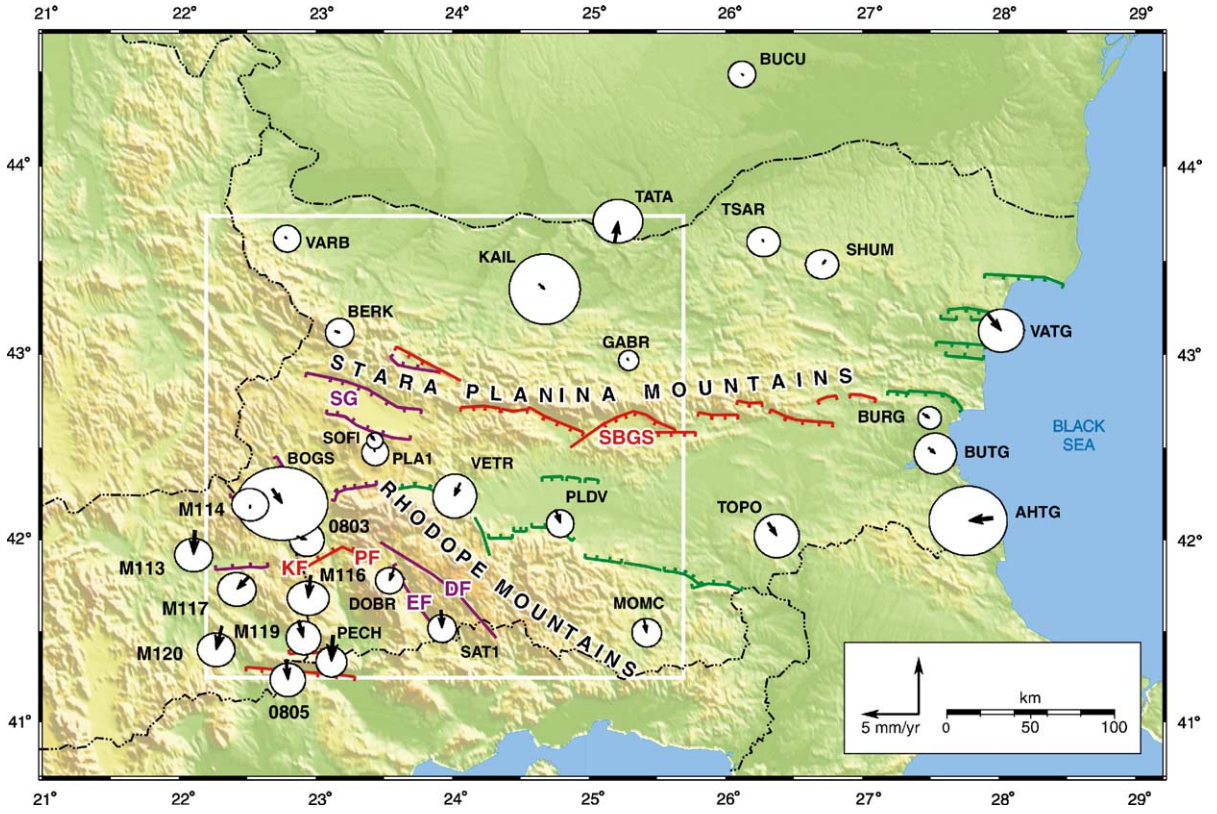

Fig. 6. Estimated velocities in the North Bulgarian-fixed reference frame (see text). Error ellipses represent regions of 95% confidence. Stations considered within the stable region of southern Romania and northern Bulgaria and used both to define the reference frame and to validate the uncertainties are BUCU, SHUM, TSAR, TATA, KAIL, GABR, and VARB (see text). Fault symbols used are same as those in Fig. 2. Colors indicate the geological evidence for recent activity (see text). DF, Dospat fault; EF, East Pirun fault; KF, Krupnik fault; PF, Predela fault; SBGS, Sub-Balkan graben system; SG, Sofia graben. The white rectangle shows the location of Fig. 7.

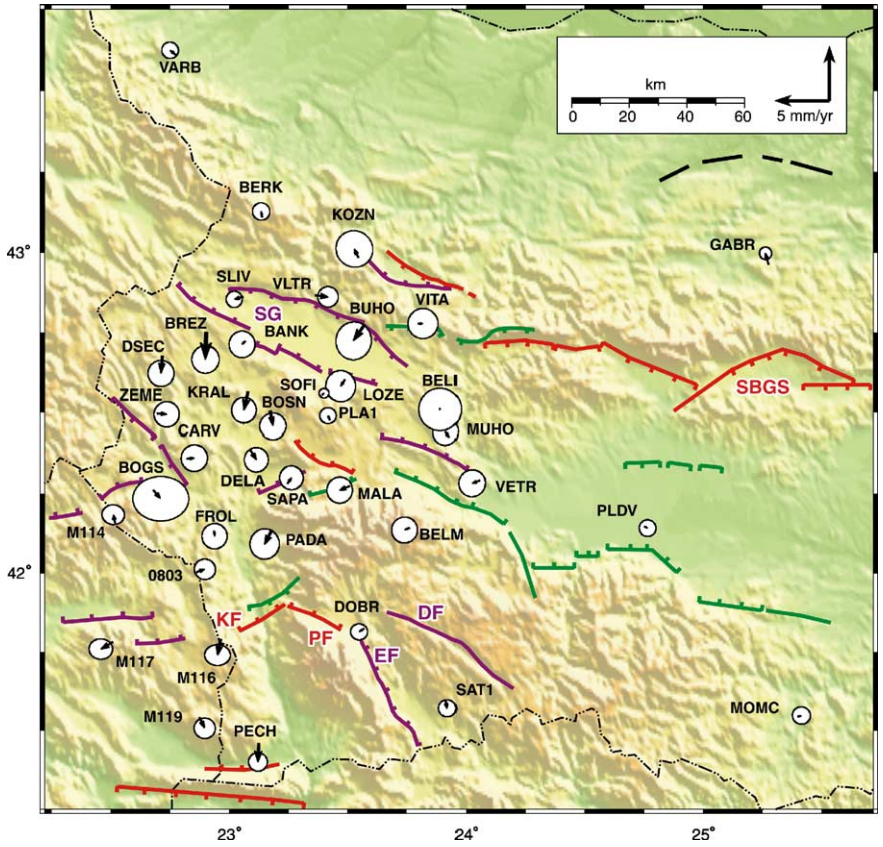

Fig. 7. Estimated velocities in the West Bulgarian-fixed reference frame, defined by the 38 stations shown in the figure. The 28 stations used to scale the uncertainties are those south of KOZN, west of GABR, and north of M116 (see text). Uncertainties are shown at 70% confidence for clarity. Stations used for the uncertainty tests include all of those in figure north of 42° except for VARB and GABR. The estimated velocity for VERI is anomalous, suggesting monument instability, so it is omitted from the plot. Fault symbols used are same as those in Fig. 2. Colors indicate the geological evidence for recent activity (see text). DF, Dospat fault; EF, East Pirun fault; KF, Krupnik fault; PF, Predela fault; SBGS, Sub-Balkan graben system; SG, Sofia graben. The location of this figure in Fig. 6 is shown by a white rectangle.

then combining these positions and their covariances to estimate velocities for the 8-year span. The combinations are performed with loose constraints on all parameters, allowing us to use generalized constraints at the end to impose a reference frame (e.g., Dong et al., 1998). The reference frame is defined in two steps (see, e.g., Steblov et al., 2003). In the first, we estimate the vector translation and rotation rates (6 parameters) which minimize the differences between our estimated horizontal velocities for 27 globally distributed stations and their velocities in the well-determined International Terrestrial Reference Frame (ITRF-2000) (Altamimi et al., 2002). In the second step, we estimate the rotation vectors for one or more groups of stations with respect to ITRF. Each group of stations may represent a truly non-deforming block (e.g., the Eurasian plate) or it may be simply a local region within which we want to view small differences in velocity. For this study, we have considered three reference frames: "Eurasia", defined by 9 stations in Europe and western Asia; "Northern Bulgaria", defined by 7 stations in northern Bulgaria; and "Western Bulgaria", defined by 23 stations in western Bulgaria and northeastern Macedonia. Velocities are shown in the Northern Bulgarian frame in Fig. 6, and in the Western Bulgarian frame in Fig. 7. Velocities in each of the three frames and a list of stations used to define them are given in Table 3.

We have attempted to determine realistic uncertainties for our velocity estimates in an iterative fashion, first computing approximate a priori uncertainties for the position estimates, then reweighting these position uncertainties based on the scatter in velocity estimates within regions for which crustal motions are small compared to the uncertainties. For this data set we applied three types of reweighting: (1) assigning an a priori uncertainty to the phase observations for each station on each day based on the observed noise in the observations; (2) adding 1 mm of random noise to the

Table 2
GPS data used

Station	1996	1997	1998	1999	2000	2001	2002	2003	2004
AHTG		177–179	253–258	223–226		223–226			
						316–318			
VATG	255–258[a]	144–149	253–260			223–226			
		175–177							
BUTG	255–258	144–149	253–258			223–226			
		177–179	177–179						
BURG	259–262	175–179	249–252			223–226			
SHUM	251–254		261–264			228–231			
						318–320			
TOPO	259–262		249–252			219–222			
TSAR	251–254		261–264			228–231			
BUCU[b]					245–257	211–239	257–263	206–207	269–270
					259–260	316–325		213–214	
								240–242	
MOMC	259–262		249–252			219–222			
GABR	251–254		261–264			228–231			269–270
TATA			269–273			232–235			
PLDV	263–266		249–252			215–218			269–270
	282–292					323–325			
KAIL	247–250		265–268			228–231			
VETR		260–263			251–254				
MUHO		263–266			254–257				
SAT1	263–266		245–248			215–218[a]			
BELI		266–269			257–260		259–261		
VITA		257–260			248–251		257–259		
BELM		257–260			248–251		261–263		
VERI		257–259			247–251				
BUHO	260–263				251–254				
DOBR	267–270	260–263	245–248		251–254	211–214			
KOZN					245–248			206–207	
MALA		254–257			245–248				
LOZE		260–263			251–254				
PLA1	247–270	141–142	261–264		254–257	211–214		213–214	
	282–292	254–269				316–325			
SOFI[b]		175–179	245–273	223–225	245–257	211–239	257–263	206–207	269–270
		254–269			259–260	316–325		213–214	
								240–242	
VLTR		263–266			254–257	236–239			
CHER[c]					257–260			240–242	
SAPA		254–257			245–248				
PADA		257–260			248–251				
BOSN		266–269			257–260				
BERK	247–250	254–257	265–268		245–248	236–239			
PECH	267–270		245–248			211–214			
DELA		263–266			254–257				
KRAL		263–266			254–257				
BANK		254–257			245–248				
SLIV		266–269			257–260		257–259		
M116[d]	225–230				274–275				
FROL		254–257			245–248		261–263		
BREZ		266–269			257–260				
M119[d]	225–230				275–276				
803[d]	225–230				273–274				
CARV		260–263			251–254				
805[d]	225–230				275–276				
VARB	247–250					236–239			
						320–322			
DSEC		266–269			257–260				

Table 2 (*continued*)

Station	1996	1997	1998	1999	2000	2001	2002	2003	2004
ZEME		263–266			254–257		259–261		
BOGS	267–270	257–260	245–248		248–251	211–214			
M114[d]	225–230				271–272				
M117[d]	225–230				270–271				
M120[d]	225–230				271–272				
M113[d]	225–230				270–271				

Numbers show start and end days of the year between which GPS data were collected continuously.
[a] A reference mark was observed instead of the main marker.
[b] Permanent IGS station (BUCU at Bucharest, Romania, SOFI near Sofia, Bulgaria).
[c] Setup problem.
[d] Station in eastern Macedonia (see Burchfiel et al., 2005—this issue).

uncertainty to the horizontal position estimated from each survey, primarily to account for oversampling of observations for continuous stations; (3) allowing 0.5 mm/year of random walk in horizontal positions to better account for temporal correlations (e.g., Williams et al., 2004). Finally, we examined the time series for all of the stations in the Balkan region with measurements at three or more epochs, removing obvious outliers and further downweighting those for which the normalized root-mean-square (nrms) scatter was greater than 1.5. Five of these time series are shown in Fig. 8. The rates and uncertainties estimated for the north and east components in the time series differ slightly from those given in Table 3 (Eurasian frame) because, unlike the full velocity solution, the time series do not account rigorously for all correlations and do not include the influence of the random walk component on the velocity estimates and uncertainties. The rate uncertainties from the time series do include the random noise added to the position uncertainties: 1 mm for SOFI, PECH, and MOMC, 2 mm for BERK and GABR. Note that the time series for GABR and MOMC indicate no significant error in our corrections for the Izmit earthquake.

Although the chi-square per degree of freedom for the velocity solution (0.4) and the median nrms from the time series for the Balkan stations (0.8) indicate a good fit to the data, neither provides an adequate basis for determining the velocity uncertainties. The overall chi-square is skewed by the statistics of the global stations and the lack of redundancy for most of the Balkan stations. Both the solution chi-square and the time-series nrms fail to account for the non-random nature of the error spectrum. Rather, we validate our weighting of the data using the consistency of the velocity scatter with what we would expect for non-deforming areas. Specifically, we examined 53 stations in three regions for which the relative velocities are small and randomly distributed: northern Bulgaria (Fig. 6), the central part of western Bulgaria (Fig. 7), and central Macedonia (Burchfiel et al., 2005—this issue, Fig. 4). When plotted with 70% confidence ellipses, the velocities of 40 of the 53 stations (75%) fall within the bounds of the ellipses; with 95% confidence ellipses, 49 fall within the bounds (93%). Strictly, uncertainties obtained in this manner are upper bounds since actual deformation may be contributing to the scatter. The apparent randomness of most of the velocities within these regions, however, suggests that any contribution from deformation is small.

When displayed with respect to the stable region of northern Bulgaria (Fig. 6), the estimated GPS velocities south of the Stara Planina Mountains show south-oriented motion at a rate of 1–2 mm/year. This motion corroborates in a broad sense the central zone of extension inferred from the geology and seismicity, though the southward motion estimated for MOMC and TOPO may be corrupted by errors in our model for the Izmit displacements. Within the dense network in the west (Fig. 7), there are three regions where the consistency in the velocities of three or more stations suggests the possibility of deformation. The small ($\sim 0.5 \pm 0.5$ mm/year) northward motion of VARB, BERK, and KOZN tends to corroborate the geological and seismic evidence for extension in the western part of the Stara Planina Mountains. In SW Bulgaria and adjacent Macedonia PETB, M119 and M116 move to the south at ~1 mm/year relative to stations to the north and east. This is consistent with N–S extension on the Krupnik fault. It would also suggest that the N–S striking East Pirin fault south of DOBR should have a component of left-lateral strike–slip for which we have no geological evidence.

The third region of apparent deformation is in the westernmost portion of the network, where DSEC, BREZ, KRAL, BOSN move consistently southward at 1–2 mm/year. This motion supports extension along the southern margin of the Sofia graben. However, it also implies shortening between these stations on structures

Table 3
GPS station velocities

Station	Lon.°E	Lat.°N	Eurasian frame				North Bulgarian frame		West Bulgarian frame	
			East (mm/year)	North (mm/year)	σEast (mm/year)	σNorth (mm/year)	East (mm/year)	North (mm/year)	East (mm/year)	North (mm/year)
Estimates from this solution										
VILL	356.05	40.44	−0.3	0.2	0.3	0.2	−1.8	5.9	−0.5	−0.3
POL2	74.69	42.68	−1.2	2.9	0.4	0.4	−2.5	−3.2	1.3	8.8
KIT3	66.89	39.14	−1.3	0.6	0.4	0.3	−2.8	−4.5	1.0	6.2
ZWEN	36.76	55.70	0.4	−0.4	0.3	0.2	3.4	−0.8	−1.0	3.3
ANKR	32.76	39.89	−20.6	−2.2	1.1	1.0	21.0	−2.0	20.2	1.1
AHTG	27.95	42.10	−2.2	−1.2	1.4	1.2	−2.1	−0.2	−2.2	1.6
VATG	27.92	43.20	0.8	−2.4	0.8	0.8	1.1	−1.4	0.7	0.5
BUTG	27.48	42.48	0.5	−1.5	0.8	0.7	0.6	−0.5	0.4	1.2
BURG	27.44	42.67	0.4	−1.4	0.4	0.4	0.6	−0.4	0.3	1.4
SHUM	26.73	43.49	−0.6	−1.5	0.6	0.5	−0.3	−0.4	−0.8	1.2
TOPO	26.31	42.08	0.7	−2.4	0.8	0.8	0.7	−1.1	0.6	0.3
TSAR	26.27	43.60	−0.3	−1.5	0.6	0.5	0.1	−0.2	−0.5	1.2
BUCU	26.13	44.46	−0.7	−1.2	0.5	0.5	−0.1	0.1	−1.0	1.5
MOMC	25.40	41.55	0.3	−2.5	0.5	0.5	0.2	−1.1	0.3	0.1
GABR	25.28	42.96	−0.1	−1.6	0.4	0.4	0.1	−0.2	−0.3	1.0
TATA	25.18	43.58	0.0	0.5	0.9	0.8	0.3	1.9	−0.3	3.1
PLDV	24.75	42.15	0.4	−2.7	0.5	0.5	0.4	−1.2	0.3	−0.1
KAIL	24.63	43.36	0.2	−2.0	1.3	1.3	0.5	−0.5	−0.1	0.6
METS	24.40	60.22	0.3	−1.1	0.2	0.2	4.1	0.5	−2.2	1.4
VETR	24.06	42.29	−0.5	−2.7	0.8	0.8	−0.5	−1.1	−0.7	−0.3
MUHO	23.93	42.43	−0.2	−2.0	0.7	0.8	−0.1	−0.4	−0.4	0.4
SAT1	23.92	41.60	0.2	−3.2	0.5	0.5	0.1	−1.6	0.1	−0.7
BELI	23.89	42.51	0.2	−2.5	1.2	1.2	0.2	−0.9	0.0	−0.1
VITA	23.80	42.78	0.7	−2.4	0.9	0.9	0.8	−0.8	0.4	0.0
BELM	23.76	42.14	−0.3	−2.6	0.8	0.8	−0.3	−1.0	−0.5	−0.2
VERI	23.73	42.48	2.6	−4.0	0.8	0.8	2.7	−2.3	2.4	−1.6
BUHO	23.57	42.77	−0.8	−3.8	1.0	1.1	−0.6	−2.2	−1.0	−1.4
DOBR	23.57	41.82	−0.3	−2.7	0.5	0.5	−0.4	−1.0	−0.4	−0.3
KOZN	23.55	42.99	−0.1	−1.7	1.1	1.1	0.1	0.0	−0.4	0.8
MALA	23.51	42.27	−0.7	−2.8	0.8	0.8	−0.7	−1.1	−0.9	−0.4
LOZE	23.49	42.60	−0.1	−3.0	0.9	0.9	−0.1	−1.3	−0.4	−0.6
PLA1	23.43	42.48	0.0	−2.0	0.5	0.5	0.1	−0.3	−0.2	0.4
SOFI	23.40	42.56	0.3	−2.3	0.3	0.3	0.4	−0.6	0.1	0.1
VLTR	23.36	42.87	1.4	−2.5	0.6	0.6	1.6	−0.8	1.2	−0.2
CHER	23.28	42.56	−1.9	−2.2	0.9	0.9	−1.8	−0.5	−2.1	0.2
SAPA	23.25	42.28	0.6	−1.9	0.7	0.7	0.6	−0.1	0.4	0.5
PADA	23.18	42.14	−0.5	−3.6	0.9	0.9	−0.5	−1.9	−0.7	−1.3
BOSN	23.17	42.51	0.5	−3.7	0.8	0.8	0.5	−2.0	0.3	−1.4
BERK	23.14	43.11	0.2	−1.9	0.5	0.5	0.4	−0.1	−0.1	0.5
PECH	23.13	41.46	0.0	−4.0	0.6	0.5	−0.2	−2.3	−0.1	−1.7
DELA	23.09	42.39	0.8	−3.3	0.7	0.7	0.8	−1.5	0.6	−0.9
KRAL	23.08	42.57	−0.2	−4.0	0.7	0.8	−0.1	−2.3	−0.4	−1.7
BANK	23.07	42.72	0.0	−2.6	0.8	0.8	0.1	−0.9	−0.3	−0.3
SLIV	23.06	42.86	−0.5	−2.6	0.5	0.5	−0.4	−0.8	−0.8	−0.2
M116	22.96	41.79	−0.2	−3.8	0.8	0.6	−0.2	−2.0	−0.3	−1.4
FROL	22.94	42.13	0.3	−2.8	0.7	0.7	0.2	−1.0	0.1	−0.5
BREZ	22.90	42.75	0.2	−4.8	0.8	0.8	0.3	−3.0	−0.1	−2.4
M119	22.88	41.54	0.6	−3.3	0.6	0.6	0.4	−1.5	0.5	−1.0
0803	22.86	42.00	0.9	−2.1	0.6	0.6	0.8	−0.3	0.7	0.3
CARV	22.82	42.36	0.9	−2.3	0.8	0.8	0.9	−0.5	0.7	0.1
0805	22.78	41.33	0.4	−3.6	0.6	0.6	0.2	−1.8	0.3	−1.2
VARB	22.77	43.61	−0.1	−1.9	0.5	0.5	0.2	−0.1	−0.5	0.4
DSEC	22.72	42.68	0.1	−3.9	0.8	0.8	0.2	−2.1	−0.1	−1.6
ZEME	22.70	42.50	1.1	−2.4	0.7	0.7	1.2	−0.6	0.9	−0.1
BOGS	22.68	42.26	0.8	−3.1	1.6	1.3	0.8	−1.3	0.6	−0.8

Table 3 (*continued*)

Station	Lon.°E	Lat.°N	Eurasian frame				North Bulgarian frame		West Bulgarian frame	
			East (mm/year)	North (mm/year)	σEast (mm/year)	σNorth (mm/year)	East (mm/year)	North (mm/year)	East (mm/year)	North (mm/year)
M114	22.52	42.16	0.1	−1.6	0.7	0.6	0.0	0.3	−0.1	0.7
M117	22.51	41.78	−0.9	−2.9	0.7	0.6	−1.0	−1.1	−1.1	−0.6
M120	22.31	41.51	−0.3	−3.9	0.7	0.6	−0.5	−2.1	−0.4	−1.6
M129	22.21	41.16	0.9	−4.3	0.6	0.6	0.6	−2.5	0.8	−2.1
M113	22.12	42.03	−0.1	−4.0	0.7	0.6	−0.1	−2.1	−0.2	−1.8
0804	22.01	41.77	0.2	−3.1	0.6	0.6	0.0	−1.2	0.0	−0.9
M104	21.93	42.31	1.4	−2.4	0.6	0.6	1.4	−0.4	1.1	−0.1
M112	21.80	41.99	−0.3	−3.3	0.7	0.7	−0.4	−1.3	−0.5	−1.0
0806	21.79	40.93	0.4	−4.2	1.1	1.0	0.1	−2.2	0.4	−1.9
M121	21.65	41.33	−0.5	−3.7	0.7	0.6	−0.7	−1.7	−0.6	−1.5
0802	21.45	42.19	1.7	−0.8	0.6	0.6	1.7	1.2	1.5	1.4
M111	21.40	41.70	−0.6	−3.4	0.8	0.8	−0.7	−1.4	−0.7	−1.2
M122	21.21	41.44	−0.2	−3.4	0.7	0.6	−0.5	−1.4	−0.4	−1.3
M127	21.18	41.00	0.6	−3.4	0.7	0.6	0.3	−1.4	0.5	−1.3
M110	21.05	41.66	0.3	−2.9	0.7	0.6	0.1	−0.9	0.1	−0.8
M125	21.03	41.23	1.7	−3.0	0.6	0.6	1.4	−1.0	1.6	−0.9
JOZE	21.03	52.10	0.2	0.1	0.3	0.3	2.2	2.2	−1.3	2.3
0807	20.82	40.93	0.0	−2.1	0.7	0.6	−0.3	0.0	−0.1	0.0
M108	20.80	41.99	0.1	−1.7	0.6	0.6	0.0	0.4	−0.1	0.4
M123	20.68	41.43	−0.6	−3.3	0.7	0.6	−0.8	−1.2	−0.7	−1.2
QTH2	20.60	41.07	1.3	−3.4	1.9	1.1	1.0	−1.3	1.2	−1.3
0801	20.54	41.77	0.3	−2.8	0.7	0.6	0.1	−0.6	0.1	−0.7
M124	20.52	41.24	−1.6	−2.2	0.6	0.6	−1.9	−0.1	−1.7	−0.1
MAQE	20.47	41.59	−0.5	−2.4	1.0	0.7	−0.7	−0.3	−0.7	−0.3
BERA	19.95	40.71	−2.8	−1.1	1.0	0.6	−3.2	1.2	−2.9	1.0
VLOR	19.51	40.41	−0.7	1.5	1.2	0.8	−1.2	3.9	−0.7	3.5
SHKO	19.50	42.05	−1.4	0.4	0.9	0.5	−1.6	2.7	−1.7	2.4
TROM	18.94	69.66	−0.6	1.0	0.3	0.3	5.0	3.4	−4.3	2.9
BOR1	17.07	52.28	0.3	0.1	0.2	0.2	2.3	2.8	−1.3	1.9
GRAZ	15.49	47.07	0.2	0.4	0.2	0.2	1.0	3.3	−0.8	1.9
POTS	13.07	52.38	−0.2	0.1	0.5	0.5	1.6	3.4	−1.9	1.5
WTZR	12.88	49.14	0.1	0.2	0.2	0.2	1.3	3.6	−1.2	1.5
ONSA	11.93	57.40	−0.7	−0.6	0.2	0.2	2.1	2.9	−3.1	0.6
NYAL	11.87	78.93	0.3	−0.8	0.3	0.3	7.1	2.7	−4.7	0.4
MEDI	11.65	44.52	1.4	2.2	0.3	0.3	1.5	5.7	0.6	3.3
GRAS	6.92	43.76	0.0	0.2	0.3	0.3	−0.2	4.4	−0.7	0.9
KOSG	5.81	52.18	0.1	0.3	0.5	0.5	1.5	4.7	−1.7	0.9
BRUS	4.36	50.80	−0.3	−0.6	0.2	0.2	0.8	4.0	−1.9	−0.2
HERS	0.34	50.87	−0.1	0.2	1.9	1.8	0.6	5.3	−1.8	0.2

(1) The uncertainties when the velocities are expressed in the North Bulgarian frame and in the West Bulgarian frame are same as those in the Eurasian frame. For all stations, the correlations between the N and E velocity estimates are less than 0.05 and hence are omitted.
(2) Stations used to realize the Eurasian-fixed frame: VILL, ONSA, ZWEN, GRAS, JOZE, BRUS, BOR1, GRAZ, WTZR.
(3) Stations used to realize the North Bulgarian-fixed frame: SHUM, TSAR, BUCU, GABR, TATA, KAIL, VARB.
(4) Stations used to realize the West Bulgarian-fixed frame: VETR, MUHO, BELI, VITA, BELM, VERI, BUHO, MALA, LOZE, PLA1, SOFI, VLTR, SAPA, PADA, BERK, BANK, SLIV, FROL, BREZ, CARV, DSEC, ZEME, M114.

to the south, for which there is no geological evidence. It is possible that these southward velocities reflect unidentified systematic errors in the GPS processing. These four stations have been surveyed only twice, three of them (DSEC, BREZ, BOSN) always together, on days 266–269 of 1997 and days 257–260 of 2000 (Table 2). Stations BELI, SLIV, and SOFI were surveyed on these days but also in other years. The time series for BELI, but not SLIV and SOFI shows position estimates for 1997 and 2000 that are consistent with a southward bias of about 1 mm/year (1.5-sigma).

5. Comparison of seismic and geodetic strain

Because of the variability of the P and T axes for each domain, and the indication that they reverse posi-

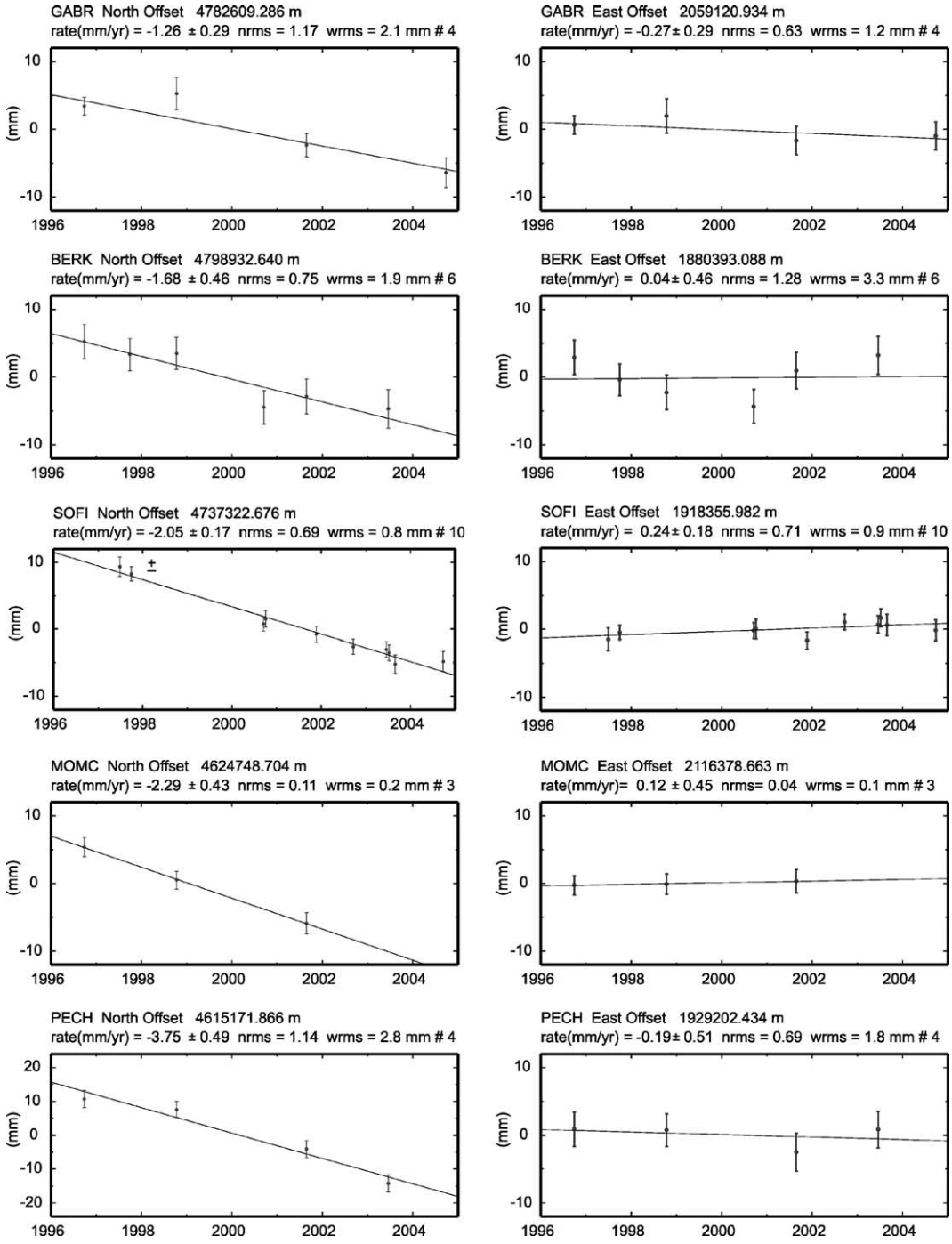

Fig. 8. Long-term repeatabilities of the horizontal station positions.

tion from near horizontal to near vertical, the analysis of the seismic data yields only a general orientation for the principal stress axes, allowing only qualitative comparison with the geodetic results. We computed surface strain from the GPS velocity solution using the technique described by Dong (1993). Strain computations involved an estimation of the velocity gradient tensor within a set of polygonal regions with GPS stations at the vertices assuming a uniform strain field at each location. In Fig. 9 we have plotted together the principal strain axes for that domain and the best fitting sector for the horizontal projections of the minimum compression

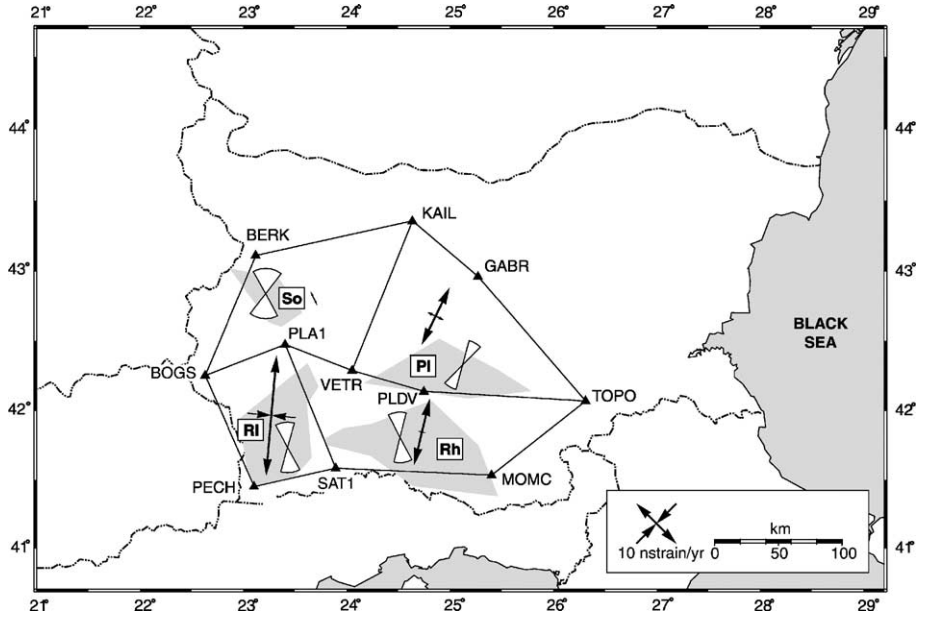

Fig. 9. Principal strain axes for polygonal regions. Strain crosses are determined from geodetic data. Data for the extensional direction from seismic data are shown by a rose diagram that includes the greatest concentration of T data points (see Fig. 5a–d) for all fault types. The rose diagrams show the uncertainty in the data set. Shaded areas show seismic domains: Pl, Plovdiv; Rh, Rhodope; Ri, Rila; So, Sofia.

axes for each seismic domain. For three of the four domains, the direction and style of the geodetically determined strains is consistent with the stress inferred from the seismic data. For the Sofia domain, it is not possible to infer a meaningful correlation. The seismic data are inadequate to determine reliably the stress state, and the geodetic data, though dense, show no significant strain in the area encompassed by the seismic data.

6. Discussion

The geological, seismological, and geodetic data are broadly consistent in identifying regions of significant extension within Bulgaria, but are not yet sufficiently quantitative to test dynamic models. To the extent that fault displacements have been dated, the geological data suggest rates of 1–2 mm/year or less, consistent with the slow present-day rates implied by the geodetic data. With several more years of high-precision GPS measurements, velocities in the current network could be estimated with uncertainties near or below 0.5 mm/year (see, e.g., McClusky et al., 2001; Friedrich et al., 2003).

In general we do not expect present-day strain rates determined from geodetic measurements to match either those inferred from seismic moment release or geological observations. Within an earthquake cycle, the velocity profile across a fault will vary in time and space depending on the viscosity of the crust (see, e.g., Meade and Hager, 2004). Moreover, if earthquakes are clustered on a 10-ky time scale, the recent seismological record will not reflect the pattern or magnitude of seismic strain release over the 10^4 to 10^6 years of faulting encompassed by our geological studies (e.g., Friedrich et al., 2003). Comparison of the strain rates inferred from the three types of observations, however, can put bounds on the geodynamic evolution and crustal rheology of the region.

7. Conclusions

Geological studies indicate the presence of numerous young and active normal faults that mostly strike E–W to WNW and are responsible for the modern topography of Bulgaria. They further suggest that the northern boundary of the Southern Balkan extensional region and hence the northern boundary of the broader Aegean extensional regime passes through central Bulgaria. Seismological and geodetic data give general support for N–S extension and yield results for some thrust faulting that has not been demonstrated from geological observations. Both geological and geodetic observations suggest that the rates of deformation are less than 2 mm/year. Longer periods of GPS observations will be necessary to correlate current strain rates with seismic activity around Sofia and other areas where there may be a significant risk of damaging earthquakes.

The analysis of the active tectonics in Bulgaria is consistent with that for Macedonia presented by Burchfiel et al. (2005—this issue), showing that the N–S extension continues westward into eastern and central Macedonia. Western Macedonia, however, shows E–W extension that continues into eastern Albania and is related to a dynamic system controlled by the northern Hellenic trench. The GPS velocities for the South Balkan extensional regime show an increase in southward velocity from Macedonia and Bulgaria into northern Greece until there is a rapid change in rate and direction across the North Anatolian fault (see Fig. 3 of Burchfiel et al., 2005—this issue). This suggests that the Aegean plate is now moving south–southwest and pulling the South Balkan lithosphere away from the region north of the South Balkan extensional regime.

Acknowledgments

This research was supported by the National Science Foundation Grant EAR-9628225, National Science Fund Grant NZ-1101/01, National Science Fund Grant NZ-608, and European Union Grant ENV4-CT95-0087. We are grateful for support in data acquisition to a personnel from the Central Laboratory of Geodesy, Bulgarian Academy of Sciences; State Department for Geodetic Survey, Skopje; Department of Geodesy of the Faculty of Construction Engineering, Tirana; Bundesamt fur Kartographie und Geodasie (BKG), Frankfurt; and the Boulder facility of UNAVCO. We obtained global solution files and most of the IGS tracking data from the Scripps Orbit and Permanent Array Center. We thank Brad Hager, Tom Herring, and Simon McClusky for helpful discussions, and Shimon Wdowinski and two anonymous reviewers for comments that have improved the manuscript. The maps in this paper were generated using the public domain Generic Mapping Tools (GMT) software (Wessel and Smith, 1995).

References

Altamimi, Z., Sillard, P., Boucher, C., 2002. ITRF2000: a new release of the International Terrestrial Reference Frame for earth science applications. J. Geophys. Res. 107 (B10), 2214. doi:10.1029/2001JB000561.

Bonchev, S., Bakalov, P., 1928. The earthquakes in southern Bulgaria of 14 and 18 April 1928 (in Bulgarian). J. Bulg. Geol. Soc. 2 (1), 58–63.

Botev, E., Samardjieva, E., Milushev, R., Dimitrov, B., Babachkova, B., Donkova, K., Alexandrova, I., Delibaltova, B., Velichkova, S., Genov, K., Hristova, C., Rizhikova, S., Toteva, T., Tzoncheva, I., 1982–2001. Preliminary data on seismic events recorded by NOTSSI (in Bulgarian with English summary). Bulg. Geophys. J. ISSN: 1311-753X.

Burchfiel, B.C., Nakov, R., Tzankov, Tz., Royden, L.H., 2000. Cenozoic extension in Bulgaria and northern Greece: the northern part of the Aegean extensional regime. In: Bozkurt, E., Winchester, J.A., Piper, J.D.A. (Eds.), Tectonics and Magmatism in Turkey and the Surrounding Area, Spec. Publ.-Geol. Soc. Lond, vol. 173, pp. 325–352.

Burchfiel, B.C., King, R.W., Todosov, A., Kotzev, V., Durmurdzanov, N., Serafimovski, T., Nurce, B., 2005. GPS results for Macedonia and its importance for the tectonics of the Southern Balkan extensional regime. Tectonophys 413, 239–248 (this issue).

Christoskov, L., Grigorova, E., 1968. On the relationship between earthquake energy and magnitude for Bulgaria. C. R. Acad. Bulg. Sci. 21 (2), 127–129.

Dong, D., 1993. The horizontal velocity field in southern California from a combination of terrestrial and space-geodetic data. PhD thesis, Mass. Inst. of Technol. Cambridge. 157 pp.

Dong, D.N., Herring, T.A., King, R.W., 1998. Estimating regional deformation from a combination of space and terrestrial data. J. Geophys. Res. 72, 200–214.

Friedrich, A.M., Wernicke, B.P., Niemi, N.A., Bennett, R.A., Davis, J.L., 2003. Comparison of geodetic and geologic data from the Wasatch region, Utah, and implications for the spectral character of Earth deformation at periods of 10 to 10 million years. J. Geophys. Res. 108 (B4), 2199. doi:10.1029/2001JB000682.

Georgiev, Tz., 1974. Fault plane solutions of two Bulgarian earthquakes. Bull. IISEE 10, 45–52.

Georgiev, Tz., 1982. Focal mechanism of the Velingrad (November 3, 1977) and Svoge earthquakes (March 9, 1980). Bulg. Geophys. J. 2 (VIII), 66–71.

Georgiev, Tz., 1987. Fault plane solutions, pressure and tension axes for some earthquakes in southwestern Bulgaria. Bulg. Geophys. J. 3 (XXIII), 102–108.

Georgiev, Tz., 1994. Seismotectonic characteristics of the dislocation line along the river valley of the Strjama. Bulg. Geophys. J. 2 (XX), 50–56.

Gephart, J.W., 1990. FMSI: a FORTRAN program for inverting fault/slickenside and earthquake focal mechanism data to obtain the regional stress tensor. Comput. Geosci. 16, 953–989.

Gephart, J.W., Forsyth, D.W., 1984. An improved method for determining the regional stress tensor using earthquake focal mechanism data: application to the San Fernando earthquake sequence. J. Geophys. Res. 89, 9305–9320.

Grigorova, E., Grigorov, B., 1964. Epicenters and Seismic Lines in Bulgaria (in Bulgarian). Bulgarian Academy of Sciences, Sofia. 83 pp.

Gutenberg, B., Richter, C.F., 1954. Seismicity of the Earth and Associated Phenomena. Princeton University Press, Princeton. 310 pp.

Herring, T.A., 2003. GLOBK: Global Kalman Filter VLBI and GPS Analysis Program Version 10.1. Mass. Inst. of Technol. Cambridge.

King, R.W., Herring, T.A., McClusky, S.C., Bock, Y., 2003. Documentation for the GAMIT GPS Software Analysis Release 10.1. Mass. Inst. of Technol. Cambridge.

Kirov, K., Grigorova, E., 1961. Seismicity of the Maritsa valley (in Bulgarian). Rep. Geophys. Inst. Bulg. Acad. Sci. 2, 37–41.

Kotzev, V., Nakov, R., Burchfiel, B.C., King, R.W., Reilinger, R., 2001a. GPS study of active tectonics in Bulgaria: results from 1996 to 1998. J. Geodyn. 31, 189–200.

Kotzev, V., Nakov, R., Burchfiel, B.C., King, R.W., 2001b. GPS constraints on the kinematics of southwestern Bulgaria. C. R. Acad. Bulg. Sci. 54 (7), 51–54.

Le Pichon, X., Angelier, J., 1979. The Hellenic arc trench system: a key to the tectonic evolution of the Eastern Mediterranean area. Tectonophysics 60, 1–42.

McClusky, S., Balassanian, S., Barka, A., Demir, C., Erginav, S., Georgiev, I., Gurkan, O., Hamburger, M., Hurst, K., Kahle, H., Kastens, K., Kekelidze, G., King, R., Kotzev, V., Lenk, O., Mahmoud, S., Mishin, A., Nadarya, M., Ouzounis, A., Paradissis, D., Peter, Y., Prilepin, M., Reilinger, R., Sanli, I., Seeger, H., Tealeb, A., Toksoz, M.N., Veis, G., 2000. Global Positioning System constraints on plate kinematics and dynamics in the eastern Mediterranean and Caucasus. J. Geophys. Res. 105, 5695–5719.

McClusky, S.C., Bjornstad, S.C., Hager, B.H., King, R.W., Meade, B.J., Miller, M.M., Monastero, F.C., Souter, B.J., 2001. Present day kinematics of the Eastern California Shear Zone from a geodetically constrained block model. Geophys. Res. Lett. 28, 3369–3372.

McKenzie, D.P., 1972. Active tectonics of the Mediterranean region. Geophys. J. R. Astron. Soc. 30, 109–185.

McKenzie, D.P., 1978. Active tectonics of the Alpine-Himalayan belt: the Aegean Sea and surrounding regions. Geophys. J. R. Astron. Soc. 55, 217–254.

Meade, B.J., Hager, B.H., 2004. Viscoelastic deformation for a clustered earthquake cycle. Geophys. Res. Lett. 31, L10610. doi:10.1029/2004GL019643.

Meyer, B., Armijo, R., Dimitrov, D., 2002. Active faulting in SW Bulgaria: possible surface rupture of the 1904 Struma earthquakes. Geophys. J. Int. 148, 246–255.

Michailovic, J., 1933. La seismicite de la Bulgarie du Sud. Monographies et travaux scientifiques Serie B. Institut Seismologique de l'Universite de Beograd, Beograd. 46 pp.

Nakov, R., Burchfiel, B.C., Tzankov, Tz., Royden, L.H., 2001. Late Miocene to Recent sedimentary basins of Bulgaria. Geol. Soc. Am. Map Chart Ser. MCH088F.

Reilinger, R., Ergintav, S., Burgmann, R., McClusky, S., Lenk, O., Barka, A., Gurkan, O., Hearn, E., Feigl, K.L, Cakmak, R., Aktug, B., Ozener, H., Toksoz, M.N., 2000. Coseismic and postseismic fault slip for the 17 August 1999, M=7.5, Izmit, Turkey earthquake. Science 289, 1519–1524.

Shanov, S., 2000. Seismotectonic model of Maritza seismic region. Rep. Geod. Warsaw Univ. Techol. 3 (48), 73–81.

Shebalin, N.V., Karnik, V., Hadzievski, D., 1974. Catalogue of Earthquakes. UNESCO, Skopje. 484 pp.

Solakov, D., Simeonova, S. (Eds.), 1993. Bulgaria Catalogue of Earthquakes 1981–1990. Bulgarian Academy of Sciences, Sofia. 39 pp.

Steblov, G., Kogan, M., King, R.W., Scholz, C.H., Burgmann, R., Frolov, D., 2003. Imprint of the North American plate in Siberia revealed by GPS. Geophys. Res. Lett. 30. doi:10.1029/2003GL017805.

Stoyanov, T., Rizikova, S., Elenkov, S., 1984. New data for the depth of the foci and density distribution of the weak earthquakes in Maritsa valley (in Bulgarian). Bulg. Geophys. J. 2 (X), 62–68.

Tzankov, Tz., Angelova, D., Nakov, R., Burchfiel, B.C., Royden, L.H., 1996. The Sub-Balkan graben system of central Bulgaria. Basin Res. 8, 125–142.

van Eck, T., Stoyanov, T., 1996. Seismotectonics and seismic hazards modeling for Southern Bulgaria. Tectonophysics 262, 77–100.

Vatsov, S., 1905. Earthquakes in Bulgaria in 1904 (in Bulgarian). Central Meteorological Survey, Sofia.

Wessel, P., Smith, W.H.F., 1995. New version of the generic mapping tools released. Eos Trans. AGU 76, 329.

Williams, S.D.P., Bock, Y., Fang, P., Jamason, P., Nikolaidis, R.M., Prawirodirdjo, L., Miller, M., Johnson, D.J., 2004. Error analysis of continuous GPS position time series. J. Geophys. Res. 109, B03412. doi:10.1029/2003/JB002741.